Kernel functions to flotation bubble size distributions

Z. Javor*, N Schreithofer and K Heiskanen*****

*Université de Lorraine, GeoRessources, CNRS, UMR 7359, 2 rue du Doyen Marcel Roubault, TSA 70605France, researcher, +33 7 68 25 52 42, zoltan-lajos.javor@univ-lorraine.fr

**Department of Chemical and Metallurgical Engineering, School of Chemical Engineering, Aalto University, Finland, researcher, +358 50 3841604, nora.schreithofer@aalto.fi

***Department of Chemical and Metallurgical Engineering, School of Chemical Engineering, Aalto University, Finland, professor emer., Outotec (Finland) Oy, Technology Director, +358 50 5552789, kari.heiskanen@outotec.com

Abstract

The physical performance of flotation excessively determined by the bubble size distribution (BSD). Although the BSD can be measured the underlying effects of different variables causing changes in dispersion and coalescence rates producing changes in the measured BSD´s is not well understood. The bubble-fluid boundary chemistry affects the coalescence rate but the details of the mechanisms are not clear, as surfactants tend to fall under some distinct types of behaviour.

We discuss the effects of volumetric coalescence rate and its effects on the BSD measured at the quiescent zones of a flotation machine. The local flow conditions, and number concentration of bubbles in an observation volume will dictate the bubble collision probability while the bubble surface curvature and the surface properties will dictate the film drainage time for a successful coalescence. This type of a model allows the separate study of the two major kernel functions (dispersion and coalescence).

Kernel functions to flotation bubble size distributions

Introduction

Flotation modelling has the challenge to combine several physicochemical phenomena into a concise model framework. The main body of modelling has been related to the well-known first order reaction model. During the years this approach with its additions and improvements has proven to be a good simple engineering model to be fitted with batch flotation data results e.g. a plug flow reactor.

$$\frac{dC}{dt} = - kC . \qquad (1)$$

The rate constant k can be obtained experimentally for any given steady-state condition. However to formulate the dependence of the rate constant from process variables has turned out to be difficult. There have been attempts to relate the rate constant to both local and global parameters (Jameson 1977) and to link the rate constant to the probabilistic bubble-particle encountering by the time averaged bubble horizontal interface flux (termed bubble surface area flux Sb) (Gorain et al., 1995a,b, 1996, 1999). To make the challenge more tractable, the total process has been generally divided into probabilistic sub-processes as outlined first by Gaudin (1932) and in more detail by Sutherland (1948). The "total probability of flotation" P_f consists of the sub-process probabilities *e.g.* particle-bubble collision P_c, attachment P_a and stability P_s (detachment)

$$k = P_f S_b . \qquad (2)$$

The flotation rate k is then modelled as a product of the "total probability of flotation" and the frequency Z that bubbles and particles interact (come so close to each other for the above mentioned sub-processes to take place *e.g*. collide).

$$ZP_f = ZP_c P_a P_s = k . \qquad (3)$$

There are several deterministic models for the particle-bubble collision (Gaudin 1932, Sutherland (1948), Yoon and Lutrell (1989), Langmuir (1948), Flint and Howarth (1971), Dukhin (1982,1983) and Dai (2000). All these models, not repeated here, are considering a single bubble-particle pair. All of them show in general a relation between the collision frequency, particle (p) and bubble size (b) as

$$E_c = A\left(\frac{p}{b}\right)^n , \qquad (4)$$

where parameter A varies from 3/2 in laminar to 3 in potential flows and n from 2 to 1, respectively.

Computational Fluid Dynamics (CFD) has become a versatile and indispensable tool to model any fluid flows containing devices and equipment, flotation devices among them. The challenges for meaningful flotation CFD are several, as the aim is to model two discrete polydisperse phases interacting in a continuous phase. Without detailing them, an important question to be asked is "*What is the bubble size to be used in flotation modelling*?"

A hypothesis to estimate bubble size has been to define a critical concentration from where added frother has no further effect on bubble coalescence (coalescence is prevented) and a minimum bubble size is reached (Cho and Laskowski, 2002). The minimum bubble size

(b_0) is attributed to machine design and operation parameters but many authors highlighted that the minimum bubble size is also affected by frother type as it can influence the bubble break-up mechanism caused by turbulent eddies in high intensity zone (Chu et al., 2016; Jávor et al., 2013; Kracht and Finch, 2009). Coalescence prevention as a determining factor of bubble size in flotation machines was questioned by Finch et al. (2008).

Population balance models (PBM) can be used in conjunction with CFD to estimate the local polydisperse phase distributions, here the bubble number density functions; NDF (Bhutani 2016). The PBM conservation equation is

$$\frac{\partial n\left(b,x,t\right)}{\partial t}+\nabla\cdot\left(\left\langle u\middle|b\right\rangle n\right)-\nabla\cdot\left(\bar{D}_x\left(b,x,t\right)\nabla n\right)=S_b\left(b,x,t\right), \qquad (5)$$

where n(b,x,t) is the number density function, b is the internal (bubble property, *e.g.* size) and x the external spatial coordinate respectively. The second and third terms on the left are the advective and diffusive parts of bubbles migrating (external coordinate space). The right hand term is the source term describing all the processes taking place in the internal coordinate space

$$S_b=B_{br}-D_{br}+B_{co}-D_{co}, \qquad (6)$$

where B_{br} and B_{co} are the birth functions due to bubble breakage and coalescence respectively. D_{br} and D_{co} are the respective death functions.

$$B_{br}\left(b\right)=\int_x^{\infty} m\left(b_1\right)a\left(b_1\right)c\left(b\middle|b_1\right)n\left(b_1\right)db_1, \qquad (7.1)$$

$$D_{br}\left(b\right)=n\left(b\right)n\left(b\right), \qquad (7.2)$$

$$B_{co}\left(b\right)=\frac{1}{\delta}\int_0^{\infty}\left(\frac{b^2}{b'^2}\right)\beta\left(b',b_1\right)n\left(b'\right)n\left(b_1\right)db_1, \qquad (7.3)$$

$$D_{co}\left(b\right)=\int_0^{\infty} b\left(b,b_1\right)n\left(b\right)n\left(b_1\right)db_1. \qquad (7.4)$$

Bubble breakage kernels $m(b_1)$, $a(b_1)$ and $c(b|b_1)$ define the number of bubbles produced in a break-up event, the frequency of break-up and the daughter distribution function respectively. Kernel $\beta(b|b_1)$ is the coalescence event frequency. This has also been divided into two parts, collision frequency and collision efficiency.

Population balance models can be solved either by the method of classes, where the NDF is discretized into a number of classes. Each class leads to an equation considering all the processes that will affect the units of the said class. The issue rising is mainly the bubble breakage and bubble coalescence. Each class would need its own kernel functions. The benefit is the natural reconstruct of the NDF. It is, however, computationally very expensive and time consuming to be used in flotation simulation. The other method to solve the bubble PBM is the method of quadrature of moments (QMOM) (McGraw 1997, Marchisio and Fox 2005, Bhutani 2017). In the method the moments of the NDF are solved from the available transported moments. As is discussed by Bhutani (2016), for an approximate estimate of NDF four moments is often sufficient. For this approach a set of kernel functions would be sufficient. This, however, requires robust kernels.

Bubble break-up and coalescence kernels have been studied extensively for bubble columns (Prince and Blanch,1990a; Luo and Svendsen,1996; Martinez-Bazan et al.,1999a,1999b,2010; Lehr and Mewes,2001; Wang et al.,2003; Zhao and Ge,2007; Liao and Lucas, 2009, 2010; Solsvik and Jakobsen,2015 among others). However, they do not take into account the effects of surfactants or solids.

Bubble break-up kernels

The Martinez-Basan (2010) model assumes that a pair of bubbles can be formed, when the stresses caused by turbulence are larger than the stresses opposing deformation at the length scales corresponding to the mother bubble. There exists always a critical bubble size at each level of turbulent intensity that cannot be broken-up.

$$b_{crit} = e^{-2/5}\left(\frac{12/}{br_s}\right)^{3/5}, \qquad (8)$$

where ε is the turbulent energy dissipation, λ_s surface tension (without surfactant), ρ the density and β a constant. The probability of break-up is (Martinez-Bazan, 2010) for a bubble with a volume V is as follows

$$P_V\left(V^*\right) \propto \left(\frac{1}{2} r b \left(e b_0\right)^{2/3}\right)^2 \left(V^{*2/9} - \mathrm{L}^{5/3}\right)\left(\left(1 - V^*\right)^{2/9} - \mathrm{L}^{5/3}\right), \qquad (9)$$

where b_0 is the mother bubble diameter, V its volume and Λ the ratio between the mother bubble size b_0 and the critical bubble size b_{crit}. The obtained bubble size distribution is (Martinez-Bazan 2010):

$$f^*\left(b^*\right) = \frac{b^{*2}\left[b^{*2/3} - \mathrm{L}^{5/3}\right]\left[\left(1 - b^{*3}\right)^{2/9} - \mathrm{L}^{5/3}\right]}{\int_{b^*_{\min}}^{b^*_{\max}} b^{*2}\left[b^{*2/3} - \mathrm{L}^{5/3}\right]\left[\left(1 - b^{*3}\right)^{2/9} - \mathrm{L}^{5/3}\right] db^*}. \qquad (10)$$

If surfactants are added to the solution in dilute concentrations their adsorption at the gas-water interface will change the surface tension in a linear way

$$/_s - / = \mathrm{G}^* RT, \qquad (11)$$

where λ_s is the surface tension without the surfactant. Γ^* is the surface concentration of the surfactant (mass of surfactant per unit area of surface). Following the linear relationship one can write for a small change in the surfactant to have an effect on the surface tension as follows (Stone and Leal,1990)

$$/^* = /_s\left(1 - j\right). \qquad (12)$$

This will change the critical bubble size of equation (8) to

$$b_{crit} = e^{-2/5}\left(\frac{12/_s\left(1 - j\right)}{br}\right)^{3/5}. \qquad (13)$$

As Martinez-Bazan et al.(2010) point out, the parameter Λ in Eq. 9 can be interpreted as the inverse of the mother bubble Weber number

$$We = \frac{r\, be^{2/3} b_0^{5/3}}{12 I^*}. \qquad (14)$$

The critical Weber number is given as 2,2 for this model (Martinez-Bazan et al 1999). The Weber number will decrease also with a factor (1-φ).

Grau et la (2005) measured the surface tensions at very low concentrations in equilibrium conditions showing the expected larger decrease in surface tension of "stronger" frothers D250 and DF1012 and a much lower decrease with D200 (Fig.11 of Grau et al.). However high speed photos taken indicate that the bubble size at the rotor is much finer with the D200 (Fig.1).

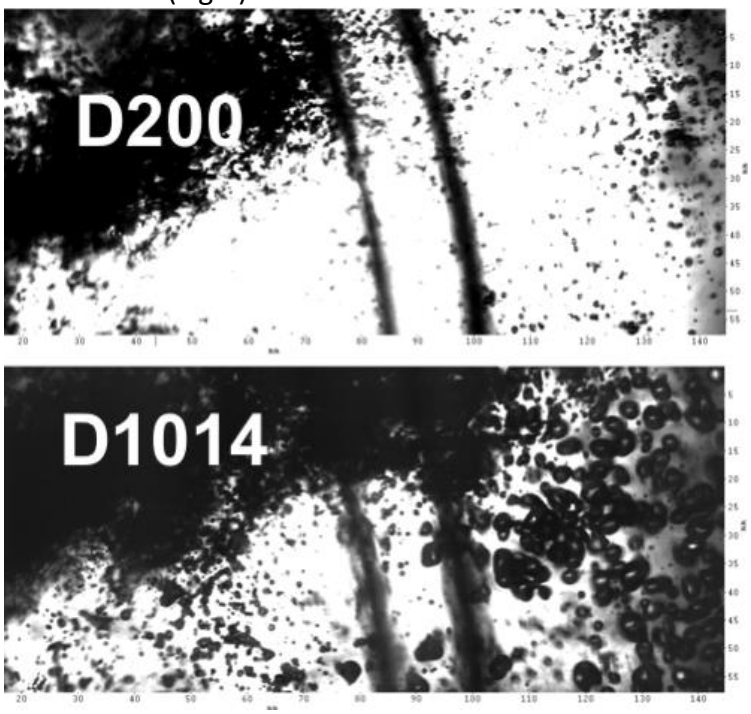


Figure 1. High speed snapshots from a 300 mm Outotec "freeflow" rotor at 20ppm frother. (water only) Courtesy Juha Tiitinen (unpublished). Pictures from bottom upwards.

Javor (2014) showed the need to use dynamic surface tension values in evaluating the correction factor in Eq. 13 instead of static values (Fig.2). Of the different frothers tested DF200 decreased the critical bubble size with about 10%, while the "stronger" frothers NF240 and DF 250 had only a marginal 2-3% decrease at very short bubble lifetimes. What is to be noted is the temporal change in NF 240 and 250 frothers. As bubbles age, the critical bubble size starts to decrease. As an outcome in a flotation cell is that after the imminent breakage of the bubbles close to the impeller, the probability of further bubble breakage diminishes rapidly. This indicates that bubble breakage kernels of the source term (Eq.5.) need to be used only in cases, where the critical bubble size is above the limit in Eq.13. The results of Javor (2014) indicate that the assumption for the velocity field to be independent from the internal coordinates (Eq.5) may not hold. There are also indications that in a turbulent field the inertia of attached bubbles create additional breakage mechanisms (Omelka et al 2009).

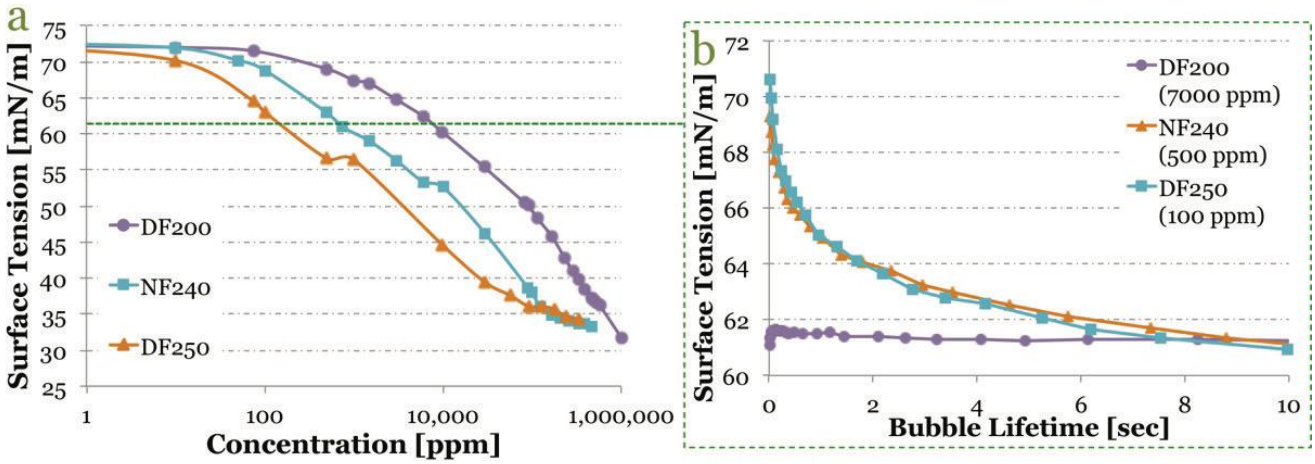


Figure 2. a) Static surface tension as a function of frother concentration and b) dynamic surface tension at equivalent static surface tension (61mN/m) concentration (Javor 2014).

Bubble coalescence kernels

In pure water gas bubbles have a tendency to coalesce as has been observed in flotation systems by Finch et al (2008). Bubble coalescence takes place in three steps (Prince and Blanch 1990). Bubbles need to collide (*e.g.* come close enough for liquid to get trapped between the bubbles). In the second phase the liquid drains away until it reaches a critical thickness. As that thickness is reached the van der Waals forces cause the film to break. There is a large body of literature discussing bubble coalescence. (Marrucci and Nicodemo 1967; Sagert et al., 1976; Derjaguin and Churaev 1978; Prince and Blanch 1990b; Marrucci 1990; Craig et al. 1993a, 1993b; Christenson and Yaminsky 1995; Deschenes et al 1998; Marcelja 2006; Henry et al., 2007; Christenson et al. 2008; del Castillo et al 2011 and others). In a simplified model we can multiply the collision rate with a success rate (Eq.15) in order to get a coalescence birth kernel for CFD modelling.

The simple equation for coalescence success rate Coulaloglou (1975) suggested is

$$p_c\left(b,b_1\right) = Exp\left(- \frac{t_{drainage}}{t_{contact}} \right). \qquad (15)$$

It relates the time the bubbles spend at a distance where the drainage of the film takes place ($t_{contact}$) to the time it takes for the film drain to a thickness where van der Waals forces rupture the thinned film ($t_{drainage}$). Machon et al (1997) added a boundary condition

$$p_c = 0, \text{ if } t_{drainage} < t_{contact}. \qquad (15b)$$

The drainage is governed by the following equations (Chesters and Hofman 1981; Carnie et al 2005), where p is hydrodynamic pressure, Π disjoining pressure, λ surface tension and μ dynamic viscosity. The notations for the terms used in equations 16-18 are presented in Fig.3.

$$Dp - \left(p + P\right) = \frac{I}{r}\frac{\partial}{\partial r}\left(r\frac{\partial h}{\partial r} \right), \qquad (16)$$

$$\frac{\partial h}{\partial t} = \frac{1}{r}\frac{\partial}{\partial r}\left[r\int_0^{h_{(r,t)}} u\left(z,t\right)dz \right], \qquad (17)$$

$$\mu\frac{\partial^2 u}{\partial z^2}=\frac{\partial p}{\partial r}. \qquad (18)$$

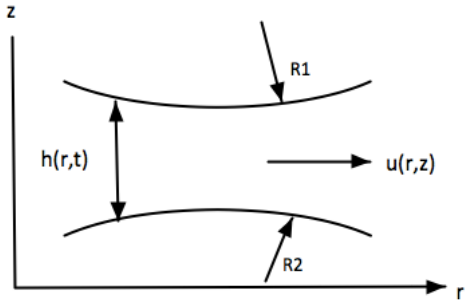


Figure 3. The notations for Eqs 16-18.

If the bubble surface is immobile then $u(z,r)_{z=h}$ =0 and the result is a parabolic Poiseuille flow

$$\frac{\partial h}{\partial t}=\frac{1}{12\mu r}\frac{\partial}{\partial r}\left(rh^3\frac{\partial p}{\partial r}\right). \qquad (19)$$

For a fully mobile surface $u(z,r)_{z=h}\neq 0$ leads to a boundary condition of $\partial u/\partial z=0$. The outcome is a plug flow profile with a four times faster rate of distance (h) diminishing than in the Poiseuille flow case.

$$\frac{\partial h}{\partial t}=\frac{1}{3\mu r}\frac{\partial}{\partial r}\left(rh^3\frac{\partial p}{\partial r}\right). \qquad (20)$$

The real situation is more complex due to surfactant concentration gradients and resulting Marangoni stresses. However such details are not rate determining in flotation CFD modeling. As a first estimate we can use viscoelasticity to define the flow regime (Fig.4). The surface-active frothers DF250 and PPG425 show marked viscoelasticity, while D200 and 1-Pentanol had viscoelasticies below the detection limit. For D250 and PPG425 Eq. 19 should be used and for D200 and 1-Pentanol Eq. 20 is to be used.

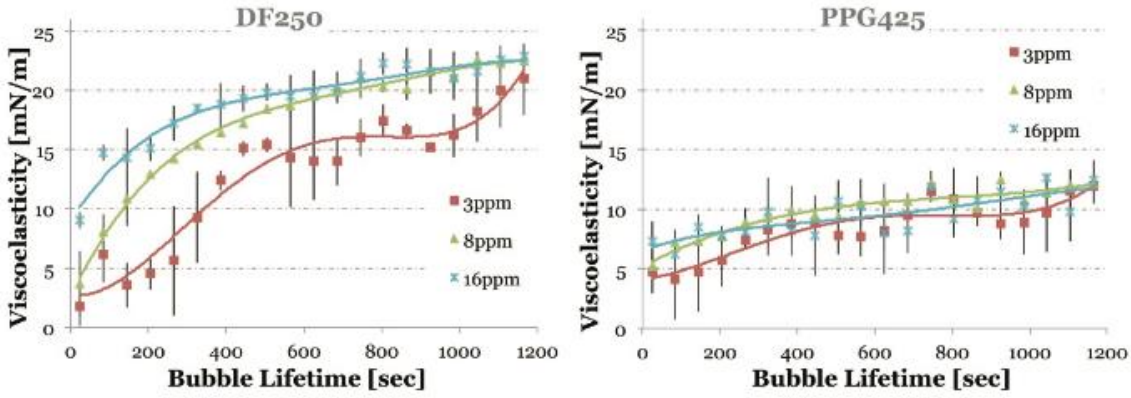


Figure 4. Viscoelasticy of DF250 and PPG425.(Javor 2014)

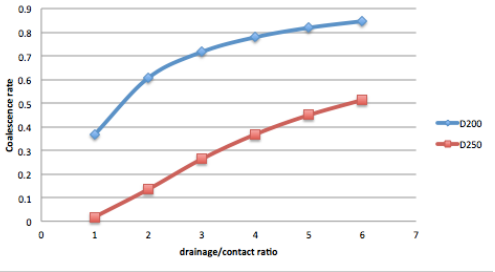


Figure 5. Difference in coalescence rates

If Eqs 19 and 20 are taken to represent the different frothers depending on their viscoelastic behavior we can see a very marked difference in the coalescence rates (Fig.5). Horn et al (2011) have mapped the effects of bubble approach velocity and NaCl concentrations on coalescence (Partially reproduced as Fig.6). Fig. 6 is intentionally left without axis values; as such data for commercial frothers is not available. The slow viscous drainage represents the immobile frother surfaces (D250 and PPF 425) and the rapid inertial drainage represents the mobile surfaces (D200 and 1-Pentanol). The study of Horn et al (2010) indicates that there exists a critical speed of approach V_c, which has an impact on the relative immobility of the surfaces (Yaminsky 2010).

$$V_c = \left(\frac{4}{3}\right)^3 \frac{(Dg)^2}{g} \frac{1}{m}, \qquad (21)$$

where $\Delta\gamma$ is the surface tension gradient from the bubble centreline outwards. The equation does not take into consideration the different behaviour of frothers, like their effects on surface viscoelasticity. The equation, however, indicates the existence of a critical bubble approach velocity.

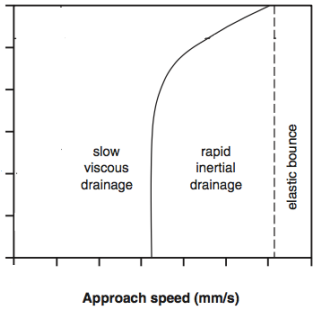


Figure 6. A partial reproduction of the Fig.2 (Horn et al 2010) with the Yaminsky critical approach velocity (Eq. 21) (Yaminsky et al 2010)

As surfactants are adsorbed onto the surface the increased rigidity of the surfaces decrease the velocity difference substantially. Clift et al (1978) showed (their Fig. 7.3) in compiling the results from several researchers that for one and two millimetre bubbles the terminal velocity difference can be in uncontaminated systems over 10 cm/s and in contaminated rigid systems 5-6 cm/s. Javor (2014) showed that different frothers had marked effects on bubble rise velocity (Fig. 7).

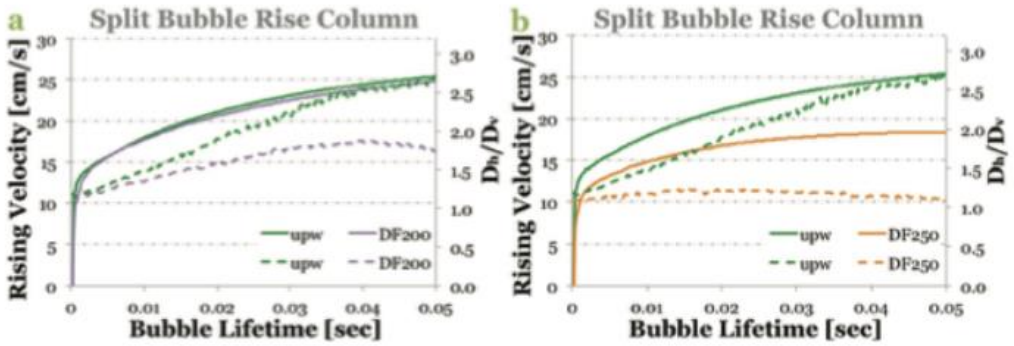


Figure 7. Rising velocity (solid line) and aspect ration (dash line) of the bubble observed in SBRC[1] a) in 8 ppm DF200; b) in 8 ppm of DF250. (Javor 2014)

There are three different mechanisms for bubbles to collide. The first is due to turbulent fluctuations. Prince and Blanch (1990) give for that probability

$$P_{CoT} = \frac{\rho}{2\sqrt{2}}\left(b_1 + b_2\right)^2 e^{1/3}\left(b_1^{2/3} + b_2^{2/3}\right)^{1/3} \qquad (22)$$

The second is due to buoyancy induced velocity differences. Liao at al (2015) gives

$$P_{cobu} = 0.5\frac{\rho}{4}\left(b_1 + b_2\right)^2 \left| v_{b1} - v_{b2} \right| \qquad (23)$$

The third mechanism is by viscous shear close to the impeller. Liao et al (2015) gives

$$P_{\text{covis}} = 0.5\frac{\rho}{4}\left(b_1 + b_2\right)^2 \left[\frac{0.5}{\rho}\left(b_1 + b_2\right) g_f\right] \qquad (24)$$

Summing up these will give the total collision probability.

$$P_{Co} = P_{coT} + P_{cobu} + P_{\text{covis}} \qquad (25)$$

The first mechanism is only related to bubble sizes and the turbulent energy dissipation. Eq. (22) assumes that bubbles take the velocity of an equal size eddy. However small eddies do not contain sufficient energy to affect bubble motion and large eddies do not generate much relative motion. Omelka et al (2009) showed that the sliding of particles on the surface of a bubble retard bubble movement in an eddy. The second mechanism is based on the assumption of a relative velocity maintained within the bubbles. Eq.25 may not capture the physical complexity of bubble-bubble collisions to a degree sufficient for modelling.

We can rewrite the coalescence kernel (Eq 7.3) by combining Eqs 15 and 25 to get

$$b\left(b,b_1\right) = P_{Co} p_c\left(b,b_1\right) = P_{Co} Exp\left(-\alpha x_p\left(V,b,b_1\right)\right), \qquad (26)$$

where α =1 for mobile surfaces and α =4 for immobile surfaces, $\xi(V,b,b_1)$ the ratio between drainage time and contact time in a pure system at an approach velocity V.

[1] In split bubble rise column (SBRC) the bubbles were released to the lower part of the column containing ultrapure water and directed the by a valve to the upper part filled with surfactant.

Conclusions

The direct use of kernel equations derived from pure systems or from studies performed with electrolytes (notably NaCl) will lead to wrong estimates of the bubble size at any spatial volume modelled. The characteristics of frothers have not been taken into consideration in the modelling of bubble behaviour. For bubble break –up it is proposed to take the frother effects into account by a correction factor dependent on the dynamic surface tension (Eq. 12 and 13). It is argued that break-up kernel computations are really needed only at volumes with high turbulent energy dissipation. However, there are indications that the presence of fine solids may bring in additional terms into the break-up kernels.

It has been shown that frothers can be divided into two major categories (for modelling purposes) based on their effects on viscoelasticity. Frothers like D200 will have a coalescence drainage behaviour best described by a plug flow of liquid, while frothers like D250 produce a parabolic Poiseuille flow. This difference in behaviour can be simplified to be taken into account in the coalescence kernel only by a constant factor of four (Eq. 26). It is acknowledged that there exists a critical bubble-bubble approach velocity, but equations derived for pure systems do not capture the phenomena taking place in flotation in such a way that they could be used in developing the kernel models.

The paper discusses some of shortcomings and outlines some of the research needs necessary to advance the quality of modelling of flotation.

References

Bhutani, G., 2016. Numerical modelling of polydispersed flows using an adaptive mesh finite element method with application to froth flotation. *Doctoral Thesis*, Imperial College, London.

Carnie, S. L., Chan, D. Y. C., Lewis, C., Manica, R., Dagastine, R. R., 2005. Measurement of dynamical forces between deformable drops using the atomic force microscope. I. Theory. *Langmuir*, ***21***, 2912–2922.

Chesters, A. K., Hofman, G., 1982, Bubble coalescence in pure liquids. *Appl. Sci. Res*., **38**, 353-361.

Cho, Y.S., Laskowski, J.S., 2002. Effect of flotation frothers on bubble size and foam stability. *Int. J. Miner. Process*. **64**, 69–80.

Christenson, H.K., Yaminsky V.V., 1995. Solute effects on bubble coalescence. *J. Phys. Chem*. **99**, 10420.

Christenson, H.K., Bowen, R.E., Carlton J.A., Denne, J.R.M, Lu, Y., 2008. Electrolytes that Show a Transition to Bubble Coalescence Inhibition at High Concentrations. *J. Phys. Chem*. *C.* **112**, 794-796.

Chu, P., Waters, K.E., Finch, J.A., 2016. Break-up in formation of small bubbles: Comparison between low and high frother concentrations. *Miner. Eng*. **96–97**, 15–19.

Clift, R., Grace. J.R, Weber. M.E., 1978. *Bubbles drops and particles*. Academic Press.

Coulaloglou, C.A., 1975. Dispersed phase interactions in an agitated flow vessel.
Ph.D. Dissertation, Illinois Institute of Technology, Chicago.

Craig, V. S. J.,Ninham, B.W., Pashley, R.M., 1993a. Effect of electrolytes on bubble coalescence. *Nature*, **364**, 317-319.

Craig, V. S. J., Ninham, B.W., Pashley, R.M., 1993b. The Effect of electrolytes on bubble coalescence in water. *J. Phys. Chem.* **97**, 10192-10197

Del Castillo, L.A., Ohnishi, S., Horn, R.G., 2011. Inhibition of bubble coalescence: Effects of salt concentration and speed of approach. *J. Colloid Interface Sci.* 356, 316–324.

Derjaguin, B.V., Churaev, N,V., 1978. On the question of determining the concept of disjoining pressure and its role in the equilibrium and flow of thin films *J Colloid Interface Sci.*, **66**,389-398.

Deschenes, L. A., Barrett, J., Muller, L. J., Fourkas, J. T., Mohanty, U., 1998. Inhibition of bubble coalescence in aqueous solutions. 1. Electrolytes. *J. Phys. Chem. B.* **102**, 5115-5119-

Finch, J. a., Nesset, J.E., Acuña, C., 2008. Role of frother on bubble production and behaviour in flotation. *Miner. Eng*. **21**, 949–957.

Fruhner, H., Wantke, K.-D., Lunkenheimer, K., 1999. Relationship between surface dilational properties and foam stability. *Colloids and Surfaces, A*, **162**, 193-202.

Gaudin, A. M., 1932. *Flotation*, McGraw-Hill, New York

Gorain, B. K., Franzidis, J.-P., and Manlapig, E. V. (1995a). Studies on impeller type, impeller speed and air flow rate in an industrial scale flotation cell. Part 1. Effect on bubble size distribution. *Miner. Eng*. **8**(6), 615–635.

Gorain, B. K., Franzidis, J.-P., and Manlapig, E. V. (1995b). Studies on impeller type, impeller speed and air flow rate in an industrial scale flotation cell. Part 2. Effect on gas holdup. *Miner. Eng*. **8**(12), 1557–1570.

Gorain, B. K., Franzidis, J.-P., and Manlapig, E. V. (1996). Studies on impeller type, impeller speed and air flow rate in an industrial scale flotation cell. Part 3. Effect on superficial gas velocity. *Miner. Eng*. **9**(6), 639–654.

Gorain, B. K., Franzidis, J.-P., and Manlapig, E. V. (1999). The empirical prediction of bubble surface area flux in mechanical flotation cells from cell design and operating data. *Miner. Eng.* **12**(3), 309–322.

Gorain, B.K., Harris, M.C., Franzidis, J., Manlapig, E. V, 1998. The effect of froth residence time on the kinetics of flotation. *Miner. Eng.* **11**, 627–638.

Grau. R., Laskowski J., Heiskanen. K., 2005. Effect of frothers on bubble size. *Int. J. Min. Proc.*, **75**, 225-233.

Henry, C.L., Dalton, C.N., Scruton, L., Craig, V.S.J., 2007. Ion-Specific Coalescence of Bubbles in Mixed Electrolyte Solutions*. J. Phys. Chem*. *C* **111**, 1015–1023.

Horn, R.G., Del Castillo, L. a., Ohnishi, S., 2011. Coalescence map for bubbles in surfactant-free aqueous electrolyte solutions. *Adv. Colloid Interface Sci*. **168**, 85–92.

Javor, Z., 2014. Frother controlled interfacial phenomena in dynamic systems – holistic approach. *Doctoral Dissertation, Aalto University Publication series; Doctoral Dissertations* 161/2014.

Jávor, Z., Schreithofer, N., Gomez, C.O., Finch, J.A., Heiskanen, K., 2013. Effect of scale dependent dynamic properties on bubble size, in: *Materials Science and Technology Conference and Exhibition 2013,* MS and T 2013.

Javor, Z., Schreithofer, N., Heiskanen, K., 2016. Multi-scale analysis of the effect of surfactants on bubble properties. *Miner. Eng.* **99**, 170–178.

Kirkpatrick, R.D., Lockett, M.J., 1974. The influence of approach velocity on bubble coalescence. *Chem. Eng. Sci.* **29**, 2363–2373.

Kracht, W. and Finch, J.A., 2009. Bubble break-up and the role of frother and salt. *Int. J. Miner. Process.* **92**, 153–161.

Langmuir I., 1948. The production of rain by a chain reaction in cumulus clouds at temperature above freezing. *J.Meteorology*, **5**(5), 175-192.

Lehr, F., and Mewes, D., 2001. A transport equation for the interfacial area density bubble columns. *Chem.Eng.Sci*. **56**, 1159–1166.

Liao, Y. , Lucas, D., 2009. A literature review of theoretical models for drop and bubble break-up in turbulent dispersions. *Chem. Eng. Sci.* **64**, 3389–3406.

Liao, Y., Lucas,D., 2010. A literature review on mechanisms and models for the coalesence process of fluid particles. *Chem. Eng. Sci*. **65**, 2851–2864.

Liao, Y., Rzehak R., Lucas, D. Krepper, E,. 2015. Baseline closure model for dispersed bubbly flow: Bubble coalescence and breakup. *Chem. Eng. Sci.* **122**, 336-349.

Luo, H., Svendsen,H.F., . Theoretical model for drop and bubble break-up in turbulent dispersions. *AIChE J*. **42**, 1225–1233.

Machon, V., Pacek, A.W., Nienow, A.W., 1997. Bubble size in electrolyte and alcohol solutions in a turbulent stirred vessel. *Trans. Inst. Chem. Eng*. **75**, 339–348.

Marcelja, S., 2006. Selective coalescence of bubbles in simple electrolytes. *J. Phys. Chem*. *B.* **110**, 13062–13067.

Marchisio, D. L., Fox R.O., 2005. Solution of population balance equations using the direct quadrature method of moments. *Aerosol Sci*. 36, 43-73.

Marrucci, G., Nicodemo, L., 1967. Coalescence of gas bubble in aqueous solutions in inorganic electrolytes. *Chem. Eng. Sci.* **22**, 1257-1265.

Marrucci, G., 1969. A theory of coalescence. *Chem. Eng. Sci.* **24**, 975–985.

Martinez-Bazan, C., Montanes J.L., Lasheras, J.C., 1999. On the break-up of an air bubble injected into a fully developed turbulent flow. Part1. Break-up frequency. *J.Fluid Mech.* **401**,157–182.

Martinez-Bazan, C., Rodriguez-Rodriguez, J., Deane, G.B., Montanes J.L., Lasheras, J.C., 2010. Considerations on bubble fragmentation models. *J.Fluid Mech.* **661**,159–177.

McGraw R., 1997. Description of Aerosol dynamics by the quadrature method of moments. *Aerosol Sci. & Tech.* **27**, 255-265.

Nesset, J.E., Finch, J.A., Gomez, C.O., 2007. Operating variables affecting the bubble size in forced air mechanical flotation machines, in: *Ninth Mill Operators' Conference 2007*. Australian Institute of Mining & Metallurgy, Fremantle, Western Australia, pp. 55–65.

Omelka, B., Schreithofer, N., Wierink, G., Heiskanen, K. 2009. Particle detachment in flotation. Proc. VI Int. Min.proc. Semin. *Santiago*, 257-262.

Prince, M.J., Blanch, H.W.,1990a. Bubble coalescence and break-up in air-sparged bubble columns. *AIChE J.* **36**,1485–1499.

Prince, M.J., Blanch, H.W.,1990b. Transition electrolyte concentrations for bubble coalescence. *AIChE J.* **36**,1425–1429.

Sagert, N.H., Quinn, M.J., Cribbs, S.C., Rosinger, L.J., 1976. Bubble coalescence in aqueous solutions of n-alcohols, in: Akers, R.R. (Ed.), *Foams*. Academic Press, INC., New York, pp. 147–162.

Solsvik, J., Jakobsen,H.A., 2015. Single air bubble break-up experiments in stirred water tank. *Int. J. Chem. React. Eng*. **10**,1–15.

Stone, H.A., Leal, L.G., 1990. The effect of surfactants on drop deformation and breakage. *J. Fluid. Mech*. **220**, 161-186

Sutherland, K. L., 1948. Physical Chemistry of flotation IX. Kinetics of the flotation process. *J. Phys. Chem,* **52**(2), 394-425.

Wang,T., Wang,J., Jin,Y., 2003. A novel theoretical break-up kernel function for bubbles/ droplets in a turbulent flow. *Chem. Eng. Sci*. **58**, 4629–4637.

Yoon, R.-H., Lutrell G.H., 1989. The effect of bubble size on fine particle flotation. *Min. Process Extr. Metall. Rev*. **5**(1&4), 101-122.

Zhao, H., Ge,W., 2007. A theoretical bubble break-up model for slurry beds or three-phase fluidized beds under high pressure. *Chem. Eng. Sci.* **62**,109–115.